

Accepted Manuscript

A moving boundary problem in a food material undergoing volume change –
Simulation of bread baking

Emmanuel Purlis, Viviana O. Salvadori

PII: S0963-9969(10)00022-0
DOI: [10.1016/j.foodres.2010.01.004](https://doi.org/10.1016/j.foodres.2010.01.004)
Reference: FRIN 3103

To appear in: *Food Research International*

Received Date: 31 July 2009
Accepted Date: 19 January 2010



Please cite this article as: Purlis, E., Salvadori, V.O., A moving boundary problem in a food material undergoing volume change – Simulation of bread baking, *Food Research International* (2010), doi: [10.1016/j.foodres.2010.01.004](https://doi.org/10.1016/j.foodres.2010.01.004)

This is a PDF file of an unedited manuscript that has been accepted for publication. As a service to our customers we are providing this early version of the manuscript. The manuscript will undergo copyediting, typesetting, and review of the resulting proof before it is published in its final form. Please note that during the production process errors may be discovered which could affect the content, and all legal disclaimers that apply to the journal pertain.

1 **A moving boundary problem in a food material undergoing volume**

2 **change – Simulation of bread baking**

3 Emmanuel Purlis^{*}, Viviana O. Salvadori

4 Centro de Investigación y Desarrollo en Criotecnología de Alimentos (CIDCA –
5 CONICET La Plata), Facultad de Ciencias Exactas, UNLP, 47 y 116, La Plata (1900),

6 Argentina

7 MODIAL, Facultad de Ingeniería, UNLP, 1 y 47, La Plata (1900), Argentina

8
9 **Abstract**

10 This paper presents a mathematical model for describing processes involving
11 simultaneous heat and mass transfer with phase transition in foods undergoing volume
12 change, i.e. shrinkage and/or expansion. We focused on processes where the phase
13 transition occurs in a moving front, such as thawing, freezing, drying, frying and
14 baking. The model is based on a moving boundary problem formulation with equivalent
15 thermophysical properties. The transport problem is solved by using the finite element
16 method and the Arbitrary Lagrangian-Eulerian method is used to describe the motion of
17 the boundary. The formulation is assessed by simulating the bread baking process and
18 comparing numerical results with experimental data. Simulated temperature and water
19 content profiles are in good agreement with experimental data obtained from bread
20 baking tests. The model well describes the stated general problem and it is expected to
21 be useful for other food processes involving similar phenomena.

22 *Keywords:* Stefan problem; Moving mesh; Coupled transport; Expansion; Shrinkage;
23 Thermophysical properties.

* Corresponding author. Phone/fax: +54 221 425 4853. E-mail: emmanuel@cidca.org.ar (E. Purlis)

24 **1. Introduction**

25

26 A large number of processes in food engineering involve simultaneous heat and
27 mass transfer (SHMT) within the product. Coupled transport is due to changes in
28 material properties with temperature and water content, as well as to gradients induced
29 by transport phenomena, e.g. a temperature gradient can generate a water content
30 gradient. In addition, the water contained in the food matrix can suffer phase change in
31 several situations. For instance, thawing and freezing involve solid-liquid transition
32 (fusion/solidification); drying (conventional, high temperature, spray-), frying and
33 baking involve liquid-vapour transition (evaporation); freeze-drying and freezing (by
34 surface dehydration) involve solid-vapour transition (sublimation). The phase transition
35 takes place in a front which is actually a moving interface. Therefore, all these processes
36 are catalogued as moving boundary problems – MBP (Farid, 2002).

37 On the other hand, changes in the volume of food, i.e. shrinkage and expansion,
38 can occur during a process involving SHMT with phase transition. Shrinkage is a
39 typical change observed during drying which happens due to loss of water and thermal
40 stress in the cellular structure of foods (Mayor & Sereno, 2004), while expansion is a
41 characteristic feature of the baking of leavened products (bread, cake). During baking,
42 thermal expansion of carbon dioxide (produced by leavening agents) and water vapour
43 present inside the porous structure deforms the dough increasing its volume until starch
44 gelatinization occurs (Lostie, Peczalski, Andrieu & Laurent, 2002). Besides the texture
45 and quality aspects related to volume change (Mayor & Sereno, 2004; Scanlon & Zghal,
46 2001), it is important from the mathematical modelling point of view to consider such
47 phenomena since the variation in the system dimensions certainly modifies the
48 temperature and water content gradients.

49 So far, few works have been published using the moving boundary analysis to
50 model food processes regarding SMHT (Campañone, Salvadori & Mascheroni, 2001;
51 Farid, 2002; Farid & Kizilel, 2009; Olguín, Salvadori, Mascheroni & Tarzia, 2008), but
52 mostly not regarding the solution of a MBP coupled with volume change. This is
53 probably due to difficulties associated with the numerical solution of this problem, the
54 lack of understanding about shrinkage and expansion phenomena and their relationship
55 with heat and mass transfer. The aim of this work was to develop a mathematical
56 formulation for describing processes involving SHMT with phase transition in foods
57 undergoing volume change. The formulation was focused on bread baking, but could be
58 applied to any of the described situations previously. The proposed model was used to
59 simulate the bread baking process under various experimental conditions, and the
60 numerical results were compared with experimental data of temperature and water
61 content.

62

63 **2. Theory**

64

65 Baking of bread is taken as the basis for developing a mathematical model for a
66 process where a wet porous food undergoes SHMT with phase transition and volume
67 change. Among the several complex changes occurring in bread during baking (Mondal
68 & Datta, 2008), the main distinguishing features are the rapid heating of bread core and
69 the development of a dry crust. The former has been explained by the evaporation-
70 condensation mechanism (Bouddour, Auriault, Mhamdi-Alaoui & Bloch, 1998; de
71 Vries, Sluimer & Bloksma, 1989; Sluimer & Krist-Spit, 1987; Wagner, Lucas, Le Ray
72 & Trystram, 2007), while the later is due to the formation and advancing of an
73 evaporation front towards the bread core (Zanoni, Peri & Pierucci, 1993; Zanoni,

74 Pierucci & Peri, 1994). Certainly, bread baking can be classified as a drying-like
75 process and therefore as a MBP. In this way, the bread can be modelled as a system
76 containing three different regions: (1) crumb: wet inner zone, where temperature does
77 not exceed 100 °C and dehydration does not occur; (2) crust: dry outer zone, where
78 temperature increases above 100 °C and dehydration takes place; (3) evaporation front:
79 between the crumb and crust, where temperature is ca. 100 °C and water evaporates
80 (liquid-vapour transition).

81 Furthermore, bread baking appears as a very particular case with respect to
82 volume change. During the process, the dough firstly undergoes a volume increase due
83 to thermal expansion of carbon dioxide and water vapour (until dough/crumb transition
84 is reached), and then shrinkage due to the final crust formation and setting, where cross-
85 linking reactions may occur (Sommier, Chiron, Colonna, Della Valle & Rouillé, 2005).
86 An additional issue of this type of MBP is the vapour diffusion throughout the dried
87 zone of the material, which is a more complicated situation than the classical MBP of
88 melting or solidification (Farid, 2002). Therefore, bread baking appears as an adequate
89 benchmark for modelling SHMT with phase transition in a wet porous food undergoing
90 volume change.

91 Mathematically, a MBP (often called as Stefan problem) is related to time-
92 dependent problems (i.e. parabolic type equations) where boundary position must be
93 determined as a function of time and space (Crank, 1987). For instance, let us consider
94 the melting of some material, in one dimension under boundary conditions of the first
95 kind; this type of problem can be formulated considering the heat balance equation for
96 each region, i.e. solid and liquid regions, with the corresponding initial and boundary
97 conditions as follows:

98 Solid region:

$$99 \quad C_1(T) \frac{\partial T}{\partial t} = \frac{\partial}{\partial x} \left(k_1(T) \frac{\partial T}{\partial x} \right), \quad 0 < x < S(t), \quad t > 0 \quad (1)$$

$$100 \quad T_1(x,0) = \varphi_1(x) \leq T_f, \quad 0 < x < S(0) \quad (2)$$

$$101 \quad T_1(0,t) = f_1(t) < T_f, \quad t > 0 \quad (3)$$

102 Liquid region:

$$103 \quad C_2(T) \frac{\partial T}{\partial t} = \frac{\partial}{\partial x} \left(k_2(T) \frac{\partial T}{\partial x} \right), \quad S(t) < x < L, \quad t > 0 \quad (4)$$

$$104 \quad T_2(x,0) = \varphi_2(x) \geq T_f, \quad S(0) < x < L \quad (5)$$

$$105 \quad T_2(L,t) = f_2(t) > T_f, \quad t > 0 \quad (6)$$

106 On the interface between solid and liquid regions, where the phase change occurs, it is
107 established that

$$108 \quad T_1(S(t),t) = T_2(S(t),t) = T_f \quad (7)$$

$$109 \quad k_2(T) \frac{\partial T_2}{\partial x} - k_1(T) \frac{\partial T_1}{\partial x} = \lambda \frac{\partial S}{\partial t} \quad (8)$$

110 This last boundary condition represents the *enthalpy jump* at the temperature of phase
111 transition. Based on a physical approach, a different mathematical formulation is
112 possible by defining an *equivalent* heat capacity per volume unit through the enthalpy
113 definition (Bonacina, Comini, Fasano & Primicerio, 1973):

$$114 \quad \tilde{C}(T) = \frac{dH(T)}{dT} = C(T) + \lambda \delta(T - T_f), \quad C(T) = \begin{cases} C_1(T), & T < T_f \\ C_2(T), & T > T_f \end{cases} \quad (9)$$

115 where $\delta(T - T_f)$ is the delta function or “Dirac function”, i.e. Eq. (9) implies that the
116 phase change occurs at temperature T_f (Bracewell, 2000). Therefore, the two-region
117 problem can be solved by only one partial differential equation with equivalent
118 coefficients that include the phase change:

$$119 \quad \tilde{C}(T) \frac{\partial T}{\partial t} = \frac{\partial}{\partial x} \left(k(T) \frac{\partial T}{\partial x} \right), \quad k(T) = \begin{cases} k_1(T), & T < T_f \\ k_2(T), & T > T_f \end{cases} \quad (10)$$

120 For a generalized and unique solution to this problem, smoothed heat capacity
 121 and thermal conductivity must be defined in order to change within a temperature range
 122 rather than at a fixed temperature (Bonacina et al., 1973). Furthermore, the delta
 123 function in Eq. (9) is replaced by a delta-type function $\delta(T - T_f, \Delta T)$ so the phase change
 124 occurs in the semi-interval ΔT across T_f , where $\delta(T - T_f, \Delta T)$ is different from zero.

125 The formulation described above is used to solve one part of the problem; the
 126 other part is related to volume variation. As was previously stated, the expansion and
 127 shrinkage occurring in bread during baking involve several complex reactions and
 128 changes (Sommier et al., 2005). All these phenomena should be included in a
 129 comprehensive mathematical model for bread baking, which finally will result in a
 130 transport problem coupled with solid mechanics to describe the volume change.
 131 Although this is a general aim to achieve, the present article deals with the specific
 132 objective of developing a mathematical formulation for solving such complicated
 133 situation, i.e. a first (necessary) step. So, the volume change is included in an empirical
 134 way: the velocity of the boundary is prescribed and described through experimental data
 135 (see Sections 2.3 and 3 for details).

136 Finally, to develop the mathematical model for bread baking, the following
 137 major assumptions were used: (1) Bread is homogeneous and continuous; the porous
 138 medium concept is included through effective or apparent thermophysical properties.
 139 (2) Heat is transported by conduction inside bread according to Fourier's law, but an
 140 effective thermal conductivity is used to incorporate the evaporation-condensation
 141 mechanism in heat transfer. Note that we are aware of the increase in the water content
 142 of the bread core this phenomenon causes, but we assume this contribution to be

143 negligible respect to the overall weight loss produced during baking (Purlis, 2007;
 144 Purlis & Salvadori, 2009a; Wagner et al., 2007). (3) Only liquid diffusion in the crumb
 145 and only vapour diffusion in the crust are assumed to occur (Luikov, 1975). (4) Water
 146 evaporates at 100 °C (non-pressurized system).

147

148 **2.1. Mathematical model for heat and mass transfer**

149

150 We consider bread as an infinite cylinder of radius R , so a one dimensional
 151 problem can be obtained from the axial symmetry assumption. We suppose that the
 152 sample has uniform temperature and water content initially. Note that since bread
 153 undergoes volume change during baking the radius R is actually not constant.

154

155 **2.1.1. Governing equations**

156

157 Heat balance equation:

$$158 \quad \rho C_p \frac{\partial T}{\partial t} = \frac{1}{r} \frac{\partial}{\partial r} \left(rk \frac{\partial T}{\partial r} \right) \quad (11)$$

159 Mass balance equation:

$$160 \quad \frac{\partial W}{\partial t} = \frac{1}{r} \frac{\partial}{\partial r} \left(rD \frac{\partial W}{\partial r} \right) \quad (12)$$

161

162 **2.1.2. Boundary conditions**

163

164 The heat arriving to the bread surface by convection and radiation is balanced by
 165 conduction inside the bread:

$$166 \quad -k \frac{\partial T}{\partial r} = h(T_s - T_\infty) + \varepsilon\sigma(T_s^4 - T_\infty^4) \quad (13)$$

167 The water migrating towards the bread surface is balanced by convective flux:

$$168 \quad -D\rho_s \frac{\partial W}{\partial r} = k_g (P_s(T_s) - P_\infty(T_\infty)) \quad (14)$$

169 where $P_s = a_w P_{sat}(T_s)$ and $P_\infty = (RH/100) P_{sat}(T_\infty)$.

170 At the centre, i.e. $r = 0$:

$$171 \quad \frac{\partial T}{\partial r} = 0 \quad (15)$$

$$172 \quad \frac{\partial W}{\partial r} = 0 \quad (16)$$

173

174 2.2. Thermophysical properties

175

176 In the MBP formulation, *equivalent* thermophysical properties are defined
 177 including the phase transition occurring during the process (water evaporation in bread
 178 baking), i.e. an equivalent property is valid for dough/crumb and crust. In this work, a
 179 smoothed Heaviside function with continuous derivative is used to incorporate the
 180 phase transition into thermophysical properties, according to previous description:

$$181 \quad \delta(y, \Delta y) = ((y_n > -1) \wedge (y_n < 1)) \times (0.5 + y_n (0.75 - 0.25 y_n^2)) + (y_n \geq 1) \quad (17)$$

$$182 \quad y_n = y / \Delta y \quad (18)$$

183 This (logical) expression approximates the step produced by phase change at T_f by
 184 smoothing the transition within the interval $-\Delta y < y < \Delta y$. In this work, $y = T - T_f$ and
 185 $\Delta y = \Delta T$, where $T_f = 100$ °C and $\Delta T = 0.5$ °C (Figure 1a). On the other hand, the delta-
 186 type function $\delta(T - T_f, \Delta T)$ describing the *enthalpy jump* is defined by the sum of two
 187 smoothed Heaviside functions with different sign (Figure 1a).

188 Following, the expressions and values for thermophysical properties of bread are
 189 briefly presented; for a detailed description, the reader is referred to Purlis (2007) and
 190 Purlis and Salvadori (2009b).

191

192 Specific heat (Figure 1b):

$$193 \quad C_p(T, W) = C_p^*(T, W) + \lambda_v W \delta(T - T_f, \Delta T) \quad (19)$$

$$194 \quad C_p^*(T, W) = C_{p,s}(T) + WC_{p,w}(T) \quad (20)$$

$$195 \quad C_{p,s} = 5T + 25 \quad (21)$$

$$196 \quad C_{p,w} = (5.207 - 73.17 \times 10^{-4} T + 1.35 \times 10^{-5} T^2) 1000 \quad (22)$$

197 Thermal conductivity (Figure 1b):

$$198 \quad k(T) = \begin{cases} \frac{0.9}{1 + \exp(-0.1(T - 353.16))} + 0.2 & \text{if } T \leq T_f - \Delta T \\ 0.2 & \text{if } T > T_f + \Delta T \end{cases} \quad (23)$$

199 Density:

$$200 \quad \rho(T) = \begin{cases} 180.61 & \text{if } T \leq T_f - \Delta T \\ 321.31 & \text{if } T > T_f + \Delta T \end{cases} \quad (24)$$

201 Density for solid (ρ_s) that appears in Eq. (14) is equal to 241.76 kg m⁻³.

202 Mass diffusivity:

$$203 \quad D(T) = \begin{cases} 1 \times 10^{-10} & \text{if } T \leq T_f - \Delta T \\ 1.32 \times 10^{-3} D_{va}(T) & \text{if } T > T_f + \Delta T \end{cases} \quad (25)$$

204 Water activity:

$$205 \quad a_w(T, W) = \left[\left(\frac{100 W}{\exp(-0.0056T + 5.5)} \right)^{-\frac{1}{0.38}} + 1 \right]^{-1} \quad (26)$$

206 The heat transfer coefficient (h) is obtained from Nusselt number correlations, and the
 207 mass transfer coefficient (k_g) is determined by using the Chilton-Colburn (or heat-mass)

208 analogy (Purlis & Salvadori, 2009b). Values for heat and mass transfer coefficients are
 209 summarized in Table 1. Respect to heat transfer by radiation, the emissivity of bread
 210 surface is considered equal to 0.9 (Hamdami, Monteau & Le Bail, 2004).

211

212 **2.3. Volume change**

213

214 The volume change is coupled to the transport model through a prescribed
 215 boundary velocity; we consider the sample radius to be a function of time, i.e. $R = R(t)$.
 216 To obtain the boundary velocity, an experimental procedure based on image processing
 217 was developed (see Section 4.2). So, the boundary velocity is calculated from the cross-
 218 section area values of bread at different times:

$$219 \quad v_b = \frac{dR_{eq}}{dt} \cong \frac{R_{eq}^{n+1} - R_{eq}^n}{t^{n+1} - t^n} \quad (27)$$

220 with

$$221 \quad R_{eq} = \sqrt{\frac{A}{\pi}} \quad (28)$$

222 Since bread samples are actually ellipsoidal rather than regular cylinders, we obtain an
 223 equivalent radius R_{eq} from the experimental data.

224

225 **3. Numerical solution**

226

227 The system of nonlinear partial differential equations describing the MBP stated
 228 in the previous section was solved using the finite element method (Zienkiewicz, 1989).
 229 The numerical procedure was implemented in COMSOL Multiphysics 3.2 (COMSOL
 230 AB, Sweden) and MATLAB 7.0 (The MathWorks Inc, USA). The Arbitrary
 231 Lagrangian-Eulerian (ALE) method was used to describe the motion of the boundary or

232 volume change of food during the process. The ALE method is an intermediate
233 approach between two classical descriptions of motion, the Lagrangian description and
234 the Eulerian description, that combines the best features of these formulations. In the
235 Lagrangian description each individual node of the mesh follows the associated material
236 particle during motion, while in the Eulerian description the mesh is fixed and the
237 continuum moves with respect to the grid. Lagrangian methods are mainly used in
238 structural mechanics, where the displacements often are relatively small. On the other
239 hand, Eulerian methods are widely used in fluid dynamics since large distortions in the
240 continuum motion can be handled with relative ease, but generally at the expense of
241 precise interface definition (Donea, Huerta, Ponthot & Rodríguez-Ferran, 2004). In the
242 ALE description, the nodes of the computational mesh may be moved in some
243 arbitrarily specified way to give a continuous rezoning capability, without the need for
244 the mesh to follow the material movement. The main advantage of the ALE method is
245 that there is no need for generating a new mesh at every time step; instead, the mesh
246 nodes are perturbed, i.e. the mesh is deformed (Duarte, Gormaz & Natesan, 2004). The
247 ALE method is popular in fluid dynamics and nonlinear solid mechanics but not in food
248 engineering; only a few articles reported the use of this approach (Białobrzewski, 2006;
249 Białobrzewski, Zielińska, Mujumdar & Markowski, 2008; Mascarenhas, Akay & Pikal,
250 1997).

251 In this work, the movement of the mesh was constrained only by a prescribed
252 boundary condition, i.e. the system was subject to free displacement. In COMSOL
253 Multiphysics, a Laplace smoothing method was applied to deform the mesh. In this
254 way, the mesh displacement was obtained by solving a partial differential equation (the
255 following explanation is valid for a general one-dimensional case):

$$256 \quad \frac{\partial^2}{\partial X^2} \left(\frac{\partial x}{\partial t} \right) = 0 \quad (29)$$

257 This equation describes a coordinate transformation between two frames or coordinate
258 systems (COMSOL AB, 2005):

259 • The spatial frame is the usual, fixed coordinate system with the spatial coordinate x .

260 In this frame the mesh is moving, i.e. the coordinate x of a mesh node is a function
261 of time.

262 • The reference frame is the coordinate system defined by the reference coordinate X .

263 In this frame the mesh is fixed to its initial position. The reference frame can be seen
264 as a curvilinear coordinate system that follows the mesh.

265 Therefore, $\frac{\partial x}{\partial t}$ represents the mesh velocity. In our model, the following boundary

266 conditions can be established to solve Eq. (29):

$$267 \quad \frac{\partial x}{\partial t} = 0, \quad X = 0 \quad (30)$$

$$268 \quad \frac{\partial x}{\partial t} = v_b(t), \quad X = L \quad (31)$$

269 So, the analytical solution for mesh velocity is:

$$270 \quad \frac{\partial x}{\partial t} = v_b(t) \frac{X}{L} \quad (32)$$

271 This equation gives also the expression to relate spatial coordinate (x) with reference
272 coordinate (X). For the present model, x represents r , while L is the initial radius of
273 bread, R_0 .

274 The solution procedure is summarized in Figure 2. The method of lines is used
275 in COMSOL Multiphysics for discretization of the partial differential equation system
276 describing the mathematical model (Eq. (11)-(26)), so a differential algebraic equation
277 system is obtained (Fletcher, 1991). This new system is solved using an implicit time-
278 stepping scheme (backward differentiation), i.e. a Newton's method together with a
279 COMSOL Multiphysics linear system solver (UMFPACK). To incorporate the volume

280 change, the solver assembles the discretized model on the deformed mesh using the
281 ALE description. For this aim, the following expression is used:

$$282 \quad \left. \frac{\partial u}{\partial t} \right|_x = \left. \frac{\partial u}{\partial t} \right|_X - \frac{\partial u}{\partial x} \frac{\partial x}{\partial t} \quad (33)$$

283 where u is a dependent variable. Eq. (33) is known as substantial or material derivative,
284 and is used to relate the Lagrangian and Eulerian approaches (Welty, Wicks & Wilson,
285 1976). Then, Eq. (32) is used to compute Eq. (33), and the partial differential equations
286 do not have to be reformulated.

287 For all simulations, the initial dimension of bread geometry was R_0 equal to 0.03
288 m, and the finite element mesh consisted in 240 elements. Relative humidity (or vapour
289 pressure) in oven ambient was assumed to be negligible. A 30 min baking process was
290 simulated for all conditions; the computing time was about 15 min using a PC with
291 AMD Phenom™ 9550 Quad-Core Processor 2.20 GHz and 4 GB RAM. The time step
292 taken by the algorithm is variable, but it was ensured to be small enough to do not miss
293 the latent heat peak corresponding to phase transition.

294

295 **4. Materials and methods**

296

297 **4.1. Bread samples**

298

299 Samples were prepared using a standard recipe for French bread: wheat flour
300 (100%), water (54.1%), salt (1.6%), sugar (1.6%), margarine (1.6%), and dry yeast
301 (1.2%). Dough was made by mixing the ingredients for 10 min in a home multi-function
302 food processor (Rowenta Universo 700 W, France) at constant speed. Then individual
303 samples of 100-150 g (cylindrical shape, ca. 0.15 m length, 0.04 m diameter) were

304 formed and placed in a perforated tray. After 1.5 h proving at ambient temperature,
305 samples duplicated approximately their volume.

306

307 **4.2. Baking tests**

308

309 Dough samples were baked in an electrical static oven (Ariston FM87-FC, Italy)
310 under two different baking conditions, depending on air velocity: natural convection (v
311 = 0 m s⁻¹) and forced convection ($v = 0.9$ m s⁻¹). Experiments were carried out by
312 duplicate using two oven temperatures: 200 and 220 °C (± 3.3 °C). Temperature inside
313 bread samples and in oven ambient was measured using T-type thermocouples (Omega,
314 USA) connected to a data logger (Keithley DASTC, USA) which was incorporated to a
315 PC; sampling time was set to 5 sec in all cases. The proving step was carried out inside
316 the oven (turn off) to avoid any movement of thermocouples while introducing the tray
317 inside the chamber. Thermocouples were placed in different positions of dough between
318 the centre and the surface along the axial axis; final locations of thermocouples were
319 determined after baking.

320 Water content was measured in five different regions along the vertical axis of
321 the central cross-section (1 cm thickness) of bread samples (Figure 3). Water content for
322 different baking times was determined by using different (but similar) samples, i.e. one
323 sample for each time. Sampling was performed every 10 min for 200 °C, and every 7
324 min for 220 °C baking temperature. Also, moisture content of unbaked dough was
325 determined. Water content values were calculated by drying the samples in a vacuum
326 oven (Gallenkamp, United Kingdom) at 80 °C, until constant weight was achieved.
327 Crust thickness was determined using a calliper in the same experiments as water

328 content. Four measures of each sample were recorded and then an average value was
329 obtained for each baking time.

330 Volume change was determined by using a computer vision system through a
331 similar protocol than for temperature measurement. At different baking times, images of
332 the cross-section of a bread sample were acquired using a digital camera (Professional
333 Series Network IP Camera Model 550710, Intellinet Active Networking, USA) and
334 processed according to the following steps (Figure 4):

335

- 336 1. Conversion of original RGB image to grey-scale format.
- 337 2. Adjustment of image intensity values to increase the contrast.
- 338 3. Noise reduction by (linear) filtering to enhance image quality.
- 339 4. Segmentation through a global threshold value: a binary image is obtained where
340 black colour (pixel value equal to 0) represents the background and white colour the
341 sample (pixel value equal to 1).
- 342 5. Measurement of cross-section area.

343

344 Image processing was performed in MATLAB. Image acquisition was
345 performed every 2 min for 200 °C, while for 220 °C, images were acquired every 1 min
346 during the first 10 min of baking, and then every 2 min for the rest of the process.
347 Additionally, to compare the influence of different patterns of volume change on heat
348 and mass transfer by simulation, an extra condition was performed. Then, volume
349 change was also measured (every 2 min) for 180 °C baking under forced convection,
350 which produces a continuous shrinkage of bread (Purlis, 2007). The obtained data was
351 used to evaluate the boundary velocity of bread (Eq. (27)) during baking by linear

352 interpolation. A detailed description of experimental procedures can be found in Purlis
353 (2007) and Purlis and Salvadori (2009a).

354

355 **5. Results and discussion**

356

357 Representative temperature profiles obtained from baking tests and numerical
358 simulation of the model are shown in Figures 5 and 6. Near the centre, temperature rises
359 until reaches 100 °C asymptotically, showing a sigmoid trend; the rapid heating of the
360 dough core has been explained through the evaporation-condensation mechanism (de
361 Vries et al., 1989; Sluimer & Krist-Spit, 1987). On the other hand, surface temperature
362 increases continuously up to 100 °C, when water evaporation occurs, and then rises
363 again towards the oven air temperature. At this location, the variation of temperature is
364 almost linear, except for the plateau accounting for phase transition (Figure 6a). Finally,
365 at the intermediate zone between the centre and the surface, the temperature increases
366 showing hybrid behaviour: it does not surpass 100 °C as the core, but the variation
367 before reaching the plateau is similar to the surface trend. As can be seen in Figures 5
368 and 6, the mathematical model predicts very well the variation of crumb temperature,
369 and reproduces the experimental trend of crust in an acceptable way. The goodness of
370 the model prediction was assessed by the mean absolute percentage error defined as
371 (Heizer & Render, 2004):

$$372 \quad e_{abs} (\%) = \frac{100}{n} \sum_{i=1}^n \left(\frac{|T_{experimental} - T_{predicted}|}{T_{experimental}} \right)_i \quad (34)$$

373 where n is the number of temperature values taken into account. The calculated
374 prediction errors corresponding to Figures 5 and 6 are summarized in Table 2.

375 Prediction errors for temperature at core and intermediate zones were between 1.16 and
376 3.18%, but were higher for the crust zone (though less than 10%).

377 Figure 7 presents typical variation of water content and crust thickness in bread
378 during baking. Outer zones of bread suffer dehydration during all the process (Figure
379 7a), which actually leads to the formation and enlargement of a dry crust (Figure 7b).
380 On the other hand, the moisture content at inner zones is almost the same as for unbaked
381 dough, throughout baking. Furthermore, we could experimentally detect an increase
382 between 0.4 and 2.3% respect to initial condition (in all experiments) that could not be
383 reproduced by simulation since it is due to the evaporation-condensation mechanism,
384 which was not included in the model. Regarding the prediction of surface moisture, the
385 model presented differences between 0.01 (at 14 and 21 min for 220 °C under natural
386 convection, and 30 min for 200 °C under forced convection) and 0.09 (at 20 min for 200
387 °C under natural convection, and 7 min for 220 °C under forced convection) kg kg^{-1} (dry
388 basis) in comparison with experimental values (Table 3).

389 The simulated values of crust thickness were computed as the distance between
390 the evaporation front and the bread surface. In this way, the position of phase transition
391 front was defined as the point where water content gradient presented a minimum
392 (Zhang & Datta, 2004). Simulation results show that the model overestimates crust
393 thickness during baking (Figure 7b and Table 3); differences were between 0.5 (at 7 min
394 for 220 °C under natural convection) and 6 (at 21 and 28 min for 220 °C under forced
395 convection) mm, which increased with baking time, and heat and mass fluxes. This can
396 be attributed to the definition of crust region used in each case, i.e. experiments and
397 simulation. In baking tests, it was determined visually as the outer dried and darker zone
398 of samples, which probably differs from the concept applied for simulation results.
399 Actually, an accurate definition of the crust is not available, being subject of study

400 currently (Vanin, Lucas & Trystram, 2009). Based on the presented results, the SHMT
401 model was validated. Differences found between experimental and simulated profiles
402 may be due to uncertainties in thermophysical properties of bread crust, such as water
403 activity, mass diffusivity, and thermal conductivity, since is the zone where occur the
404 most significant changes in temperature and water content during baking (Zhang &
405 Datta, 2006). In addition, monitoring the dynamics in the crust during the process is a
406 difficult task (Purlis & Salvadori, 2009b, Vanin et al., 2009).

407 From a general point of view, the proposed mathematical model properly
408 describes a moving boundary problem with SHMT. Figure 8 shows typical local
409 temperature and water content profiles (between centre and surface) obtained by
410 simulation (note that the boundary is moving due to volume change), which are similar
411 to the ones observed during other processes where the phase transition occurs in a
412 moving interface, e.g. drying, frying, heating of materials with high moisture, freezing,
413 thawing (Datta, 2007; Farid, 2002; Farid & Kizilel, 2009). In such situations, two
414 different regions are well defined once the temperature of phase transition has been
415 reached: a region with uniform values or smooth profiles of temperature and moisture,
416 and a zone with marked profiles of these variables. In the case of bread baking, such
417 regions are the crumb and the crust, respectively. Then, these zones are separated by the
418 phase transition front: Figure 9 shows the position of evaporation front for an arbitrary
419 simulated condition. A physical criterion to determine the position of the phase change
420 moving front is to identify the zone where a sharp change occurs in temperature or
421 water content of the product (Vanin et al., 2009). As can be seen in Figure 9, the
422 proposed model is in agreement with this definition.

423 As was previously explained, the volume change occurring during the process
424 was simulated through experimental data obtained in baking tests (Figure 10a). Note

425 that the assumption of describing the volume change by the variation in the cross-
426 section area is adequate since the axial expansion is negligible respect to change
427 occurring in the cross-section (Sommier et al., 2005). It was not the objective of this
428 work to explain the behaviour observed for different baking conditions regarding
429 volume change, since the expansion and shrinkage of bread are very complex and
430 specific phenomena. However, we can say that depending on heat and mass transfer
431 fluxes, thermal expansion and structure stiffening will develop and interact in different
432 ways leading to diverse volume change variations. For numerical solution of the model,
433 the finite element mesh was deformed applying a Laplace smoothing, so the mesh
434 velocity was described by Eq. (32). Figure 10b illustrates how a mesh consisting in
435 seven nodes (for simplicity) is deformed with time, according to volume change
436 observed in 220 °C baking under forced convection. Solving Eq. (32), it can be stated
437 that displacement of nodes is a linear function of spatial coordinate, so the displacement
438 of nodes increases from the centre to surface (Figure 10b).

439 As a summary, Figure 11 shows the evolution of bread composition, in terms of
440 crumb and crust, along baking. In other words, Figure 11 represents the objective of the
441 present paper: it describes a moving boundary problem in a food material undergoing
442 volume change. The proportion crumb/crust depends on simultaneous heat and mass
443 transfer that determines the position and advancing of the evaporation front. At the same
444 time, the volume of the product is changing according to specific mechanisms of
445 expansion and shrinkage.

446 Finally, the influence of volume change on heat and mass transfer was studied
447 by simulation of bread baking at 220 °C under forced convection for three different
448 conditions: (1) considering the actual volume change; (2) neglecting volume change
449 (i.e. fixed mesh); (3) assuming a continuous shrinkage, which was measured in other

450 condition as described in Section 4.2 (Figure 10a). Then, we focused on temperature
451 profile of the core to do the analysis (Figure 12). The different patterns of volume
452 change produced different temperature profiles due to the modification of temperature
453 gradient. Considering the experimental profile as reference, the following predictions
454 errors (Eq. (34)) were calculated for tested conditions: (1) 2.32% (SD = 2.19); (2)
455 4.04% (SD = 4.16); (3) 5.64% (SD = 5.67). In the studied case, differences could result
456 negligible from a technological point of view, but it should be note that volume change
457 certainly influences transport phenomena and the magnitude will depend on each
458 particular process.

459

460 **6. Conclusions**

461

462 Several food processes can be represented by a moving boundary problem with
463 simultaneous heat and mass transfer and volume change. In this work we developed a
464 mathematical formulation to solve numerically this general problem and the proposed
465 approach was successfully applied for simulation of bread baking. The general problem
466 involves two aspects: transport phenomena and variable domain. The former was solved
467 by a moving boundary formulation while the later through the Arbitrary Lagrangian-
468 Eulerian method. The proposed approach gives the possibility of handling simple
469 equations with continuous equivalent thermophysical properties, valid for the entire
470 operating range, where no empirical parameters or imposed or fictitious boundary
471 conditions are used to determine the position of the phase transition front. Though the
472 volume change was included in an empirical way in this work, the formulation can be
473 coupled with any other model describing expansion or shrinkage of material. For

474 example, solid mechanics can be used to model volume change of bread during baking
475 (this problem will be focus of future work).

476

477 **Acknowledgments**

478

479 Authors would like to thank to Eng. Sandro M. Goñi for helpful discussion when
480 preparing the manuscript. This research was supported by grants from Consejo Nacional
481 de Investigaciones Científicas y Técnicas (CONICET), Agencia Nacional de Promoción
482 Científica y Tecnológica (ANPCyT, PICT 2007-01090), and Universidad Nacional de
483 La Plata (UNLP) from Argentina.

ACCEPTED MANUSCRIPT

484 **Nomenclature**

485

486 A Cross-section area, m^2 487 a_w Water activity488 \tilde{C} Equivalent heat capacity, $\text{J m}^{-3} \text{K}^{-1}$ 489 C Heat capacity, $\text{J m}^{-3} \text{K}^{-1}$ 490 C_p Specific heat, $\text{J kg}^{-1} \text{K}^{-1}$ 491 D Water (liquid or vapour) diffusion coefficient of product, $\text{m}^2 \text{s}^{-1}$ 492 D_{va} Water vapour diffusion coefficient in air, $\text{m}^2 \text{s}^{-1}$ 493 e_{abs} Mean absolute percentage error, %494 f Surface temperature, K495 H Enthalpy, J m^{-3} 496 h Heat transfer coefficient, $\text{W m}^{-2} \text{K}^{-1}$ 497 k Thermal conductivity, $\text{W m}^{-1} \text{K}^{-1}$ 498 k_g Mass transfer coefficient, $\text{kg Pa}^{-1} \text{m}^{-2} \text{s}^{-1}$ 499 L Characteristic length, m500 P Water vapour pressure, Pa501 R, r Radius, m502 RH Relative humidity, %503 S Interface position, m504 SD Standard deviation505 T Temperature, K506 t Time, s507 u Dependent variable, Eq. (33)508 v_b Boundary velocity, m s^{-1}

509	W	Water (liquid or vapour) content, kg kg^{-1}
510	X	Reference coordinate, m
511	x	Spatial coordinate, m
512	y	Input of delta function, Eq. (17)-(18)
513		
514	Greek symbols	
515	δ	Delta function
516	ΔT	Temperature range of phase change, K
517	ε	Emissivity
518	λ	Heat of phase change, J m^{-3}
519	λ_v	Latent heat of evaporation, J kg^{-1}
520	ρ	Density, kg m^{-3}
521	σ	Stefan-Boltzmann constant, $5.67 \times 10^{-8} \text{ W m}^{-2} \text{ K}^{-4}$
522	φ	Initial temperature distribution, K
523		
524	Subscripts	
525	0	Initial
526	1	Solid region
527	2	Liquid region
528	∞	Ambient
529	eq	Equivalent
530	f	Phase change
531	s	Solid or surface
532	sat	Saturated
533	w	Water

534 **References**

535

536 Białobrzewski, I. (2006). Simulation of changes in the density of an apple slab during
537 drying. *International Communications in Heat and Mass Transfer*, 33 (7), 880-
538 888.

539 Białobrzewski, I., Zielińska, M., Mujumdar, A. S., & Markowski, M. (2008). Heat and
540 mass transfer during drying of a bed of shrinking particles – Simulation for
541 carrot cubes dried in a spout-fluidized-bed drier. *International Journal of Heat
542 and Mass Transfer*, 51 (19-20), 4704-4716.

543 Bonacina, C., Comini, G., Fasano, A., & Primicerio, M. (1973). Numerical solution of
544 phase-change problems. *International Journal of Heat and Mass Transfer*, 16
545 (10), 1825-1832.

546 Bouddour, A., Auriault, J.-L., Mhamdi-Alaoui, M., & Bloch, J. F. (1998). Heat and
547 mass transfer in wet porous media in presence of evaporation-condensation.
548 *International Journal of Heat and Mass Transfer*, 41 (15), 2263-2277.

549 Bracewell, R. (2000). *The Fourier transform and its applications* (3rd ed.). New York:
550 McGraw-Hill.

551 Campañone, L. A., Salvadori, V. O., & Mascheroni, R. H.(2001). Weight loss during
552 freezing and storage of unpackaged foods. *Journal of Food Engineering*, 47 (2),
553 69-79.

554 COMSOL AB (2005). *COMSOL Multiphysics Modeling Guide*. Sweden: COMSOL
555 AB.

556 Crank, J. (1987). *Free and moving boundary problems*. UK: Oxford University Press.

- 557 Datta, A. K. (2007). Porous media approaches to studying simultaneous heat and mass
558 transfer in food processes. II: Property data and representative results. *Journal of*
559 *Food Engineering*, 80 (1), 96-110.
- 560 de Vries, U., Sluimer, P., & Bloksma, A. H. (1989). A quantitative model for heat
561 transport in dough and crumb during baking. In N. G. Asp, *Cereal Science and*
562 *Technology in Sweden*, (pp. 174-188). Sweden: Lund University Chemical
563 Centre.
- 564 Donea, J., Huerta, A., Ponthot, J.-Ph., & Rodríguez-Ferran, A. (2004). Arbitrary
565 Lagrangian-Eulerian methods. In E. Stein, R. de Borst & T. J. R. Hughes,
566 *Encyclopedia of Computational Mechanics, Volume 1: Fundamentals*, (Chapter
567 14). UK: John Wiley & Sons, Ltd.
- 568 Duarte, F., Gormaz, R., & Natesan, S. (2004). Arbitrary Lagrangian-Eulerian method
569 for Navier-Stokes equations with moving boundaries. *Computer Methods in*
570 *Applied Mechanics and Engineering*, 193 (45-47), 4819-4836.
- 571 Farid, M. (2002). The moving boundary problems from melting and freezing to drying
572 and frying of food. *Chemical Engineering and Processing*, 41 (1), 1-10.
- 573 Farid, M., & Kizilel, R. (2009). A new approach to the analysis of heat and mass
574 transfer in drying and frying of food products. *Chemical Engineering and*
575 *Processing: Process Intensification*, 49 (1), 217-223.
- 576 Fletcher, C. A. J. (1991). *Computational techniques for fluid dynamics 1: Fundamentals*
577 *and general techniques* (2nd ed.). Germany: Springer-Verlag.
- 578 Hamdami, N., Monteau, J.-Y., & Le Bail, A. (2004). Heat and mass transfer in par-
579 baked bread during freezing. *Food Research International*, 37 (5), 477-488.
- 580 Heizer, J., & Render, B. (2004). *Principles of operations management* (5th ed.). New
581 Jersey: Prentice Hall.

- 582 Lostie, M., Peczalski, R., Andrieu, J., & Laurent, M. (2002). Study of sponge cake
583 batter baking process. Part I: experimental data. *Journal of Food Engineering*,
584 *51* (2), 131-137.
- 585 Luikov, A. V. (1975). Systems of differential equations of heat and mass transfer in
586 capillary-porous bodies (review). *International Journal of Heat and Mass*
587 *Transfer*, *18* (1), 1-14.
- 588 Mascarenhas, W. J., Akay, H. U., & Pikal, M. J. (1997). A computational model for
589 finite element analysis of the freeze-drying process. *Computer Methods in*
590 *Applied Mechanics and Engineering*, *148* (1-2), 105-124.
- 591 Mayor, L., & Sereno, A. M. (2004). Modelling shrinkage during convective drying of
592 food materials: A review. *Journal of Food Engineering*, *61* (3), 373-386.
- 593 Mondal, A., & Datta, A. K. (2008). Bread baking – A review. *Journal of Food*
594 *Engineering*, *86* (4), 465-474.
- 595 Olguín, M. C., Salvadori, V. O., Mascheroni, R. H., & Tarzia, D. A. (2008). An
596 analytical solution for the coupled heat and mass transfer during the freezing of
597 high-water content materials. *International Journal of Heat and Mass Transfer*,
598 *51* (17-18), 4379-4391.
- 599 Purlis, E. (2007). *Simulación de las transferencias simultáneas de materia y energía en*
600 *el proceso de horneado de pan mediante elementos finitos*. PhD thesis,
601 Universidad Nacional de Quilmes, Argentina.
- 602 Purlis, E., & Salvadori, V.O. (2009a). Bread baking as a moving boundary problem.
603 Part 1: Mathematical modelling. *Journal of Food Engineering*, *91* (3), 428-433.
- 604 Purlis, E., & Salvadori, V.O. (2009b). Bread baking as a moving boundary problem.
605 Part 2: Model validation and numerical simulation. *Journal of Food*
606 *Engineering*, *91* (3), 434-442.

- 607 Scanlon, M. G., & Zghal, M. C. (2001). Bread properties and crumb structure. *Food*
608 *Research International*, 34 (10), 841-864.
- 609 Sluimer, P., & Krist-Spit, C. E. (1987). Heat transport in dough during the baking of
610 bread. In I. D. Morton, *Cereals in a European Context*, (pp. 355-363). Chicester,
611 UK: Ellis Horwood Ltd.
- 612 Sommier, A., Chiron, H., Colonna, P., Della Valle, G., & Rouillé, J. (2005). An
613 instrumented pilot scale oven for the study of French bread baking. *Journal of*
614 *Food Engineering*, 69 (1), 97-106.
- 615 Vanin, F. M., Lucas, T., & Trystram, G. (2009). Crust formation and its role during
616 bread baking. *Trends in Food Science & Technology*, 20 (8), 333-343.
- 617 Wagner, M. J., Lucas, T., Le Ray, D., & Trystram, G. (2007). Water transport in bread
618 during baking. *Journal of Food Engineering*, 78 (4), 1167-1173.
- 619 Welty, J. R., Wicks, C. E., & Wilson, R. E. (1976). *Fundamentals of momentum, heat,*
620 *and mass transfer* (2nd ed.). New York: John Wiley & Sons.
- 621 Zandoni, B., Peri, C., & Pierucci, S. (1993). A study of the bread-baking process. I: A
622 phenomenological model. *Journal of Food Engineering*, 19 (4), 389-398.
- 623 Zandoni, B., Pierucci, S., & Peri, C. (1994). Study of the bread baking process – II.
624 Mathematical modelling. *Journal of Food Engineering*, 23 (3), 321-336.
- 625 Zhang, J., & Datta, A. K. (2004). Some considerations in modeling of moisture
626 transport in heating of hygroscopic materials. *Drying Technology*, 22 (8), 1983-
627 2008.
- 628 Zhang, J., & Datta, A. K. (2006). Mathematical modeling of bread baking process.
629 *Journal of Food Engineering*, 75 (1), 78-89.
- 630 Zienkiewicz, O. C. (1989). *The finite element method*. New York: McGraw-Hill.

631 **Figure captions**

632

633 **Figure 1.** (a) Smoothed Heaviside function (in blue) used to incorporate the phase
634 transition into thermophysical properties according to description in Section 2.2. In Eq.
635 (17) and (18), $y = T - T_f$ and $\Delta y = \Delta T$, with $T_f = 100$ °C and $\Delta T = 0.5$ °C. The delta-type
636 function $\delta(T - T_f, \Delta T)$ is used to describe the enthalpy jump (in red). (b) Typical
637 variation of thermal conductivity (k , in blue) and specific heat (C_p , in red) of bread
638 during baking (obtained from simulation at 200 °C under forced convection).

639

640 **Figure 2.** Block diagram of the numerical solution procedure described in Section 3.
641 PDE: partial differential equations; BC: boundary conditions; SHMT: simultaneous heat
642 and mass transfer; FEM: finite element method; DAE: differential algebraic equations;
643 ALE: arbitrary Lagrangian-Eulerian.

644

645 **Figure 3.** Sampling regions for determination of water content distribution in bread
646 during baking. The schema represents the central cross-section (1 cm thickness) in the
647 axial direction of bread.

648

649 **Figure 4.** Measurement of cross-section area of bread by image processing. (a) Original
650 RGB image of a sample (front view). (b) Binary image obtained by segmentation after
651 grey-scale transformation, intensity adjustment and filtering stages.

652

653 **Figure 5.** Experimental (symbols) and simulated (lines) temperature profiles at different
654 zones of bread, i.e. core (squares), intermediate (circles) and surface (triangles), during

655 baking at 200 °C under (a) natural convection and (b) forced convection. Experimental
656 values every 1 min are shown for simplicity.

657

658 **Figure 6.** Experimental (symbols) and simulated (lines) temperature profiles at different
659 zones of bread, i.e. core (squares), intermediate (circles) and surface (triangles), during
660 baking at 220 °C under (a) natural convection and (b) forced convection. Experimental
661 values every 1 min are shown for simplicity.

662

663 **Figure 7.** (a) Water content and (b) crust thickness of bread during baking at 220 °C
664 under natural convection. In (a): squares and dash line account for crumb, and triangles
665 and continuous line correspond to crust. Symbols and lines represent experimental and
666 simulated data, respectively.

667

668 **Figure 8.** Simulated (a) temperature and (b) water content profiles during baking at 220
669 °C under natural convection for different times (min): 7 (black), 14 (blue), 21 (green),
670 and 28 (red).

671

672 **Figure 9.** Simulated temperature and water content profiles corresponding to 28 min
673 baking at 220 °C under natural convection. Evaporation front position is calculated
674 according to Zhang and Datta (2004).

675

676 **Figure 10.** (a) Relative equivalent radius, i.e. $R_{eq}(t)/R_{eq}(t = 0)$, of bread during baking.
677 Triangles represent 200 °C and circles represent 220 °C oven temperature. Filled
678 symbols show natural convection and empty symbols show forced convection
679 condition. Squares account for 180 °C baking under forced convection. (b) Deformation

680 with time of a seven-node mesh according to volume change observed during baking at
681 220 °C under forced convection.

682

683 **Figure 11.** Variation of bread boundary and evaporation front positions during baking
684 at 220 °C under forced convection obtained from simulation.

685

686 **Figure 12.** Core temperature profiles at bread during baking at 220 °C under forced
687 convection. Lines correspond to different simulated conditions for volume change: thick
688 line for actual volume change, normal line for fixed mesh, and dashed line for
689 continuous shrinkage. Circles represent experimental data.

ACCEPTED MANUSCRIPT

Figure 1 – Purlis and Salvadori

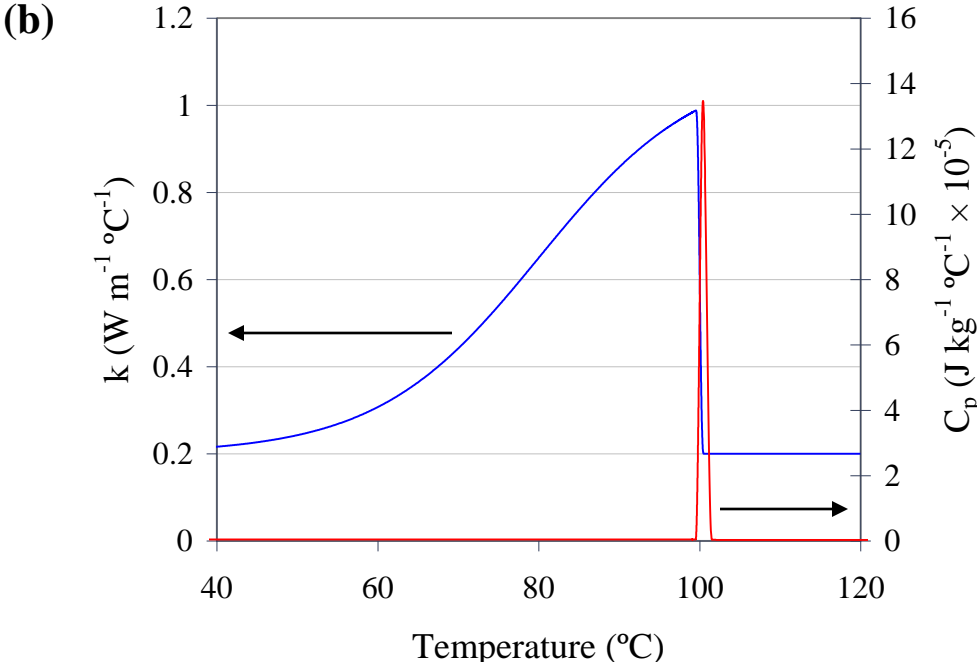
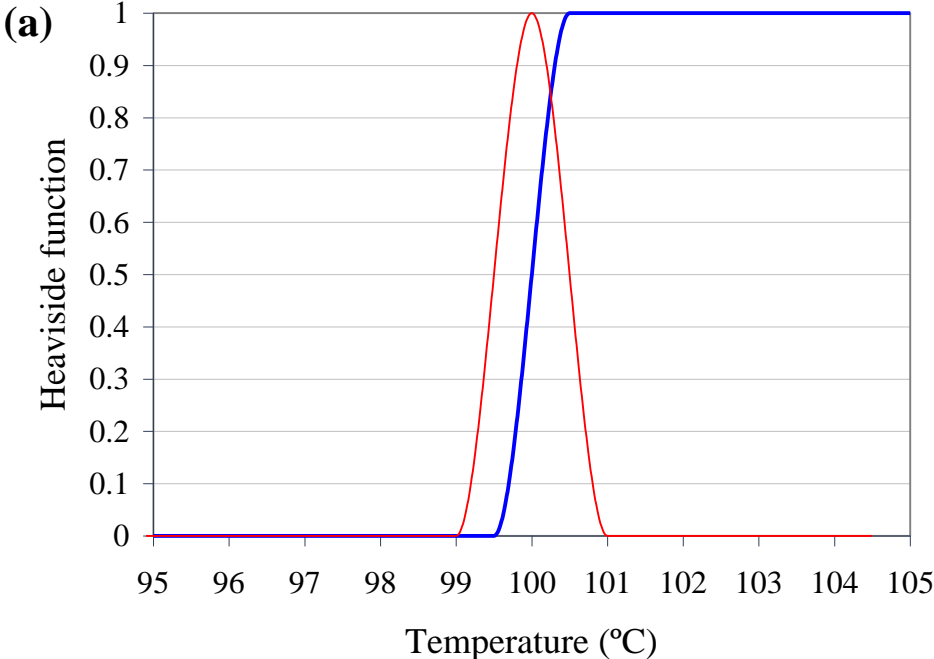


Figure 2 – Purlis and Salvadori

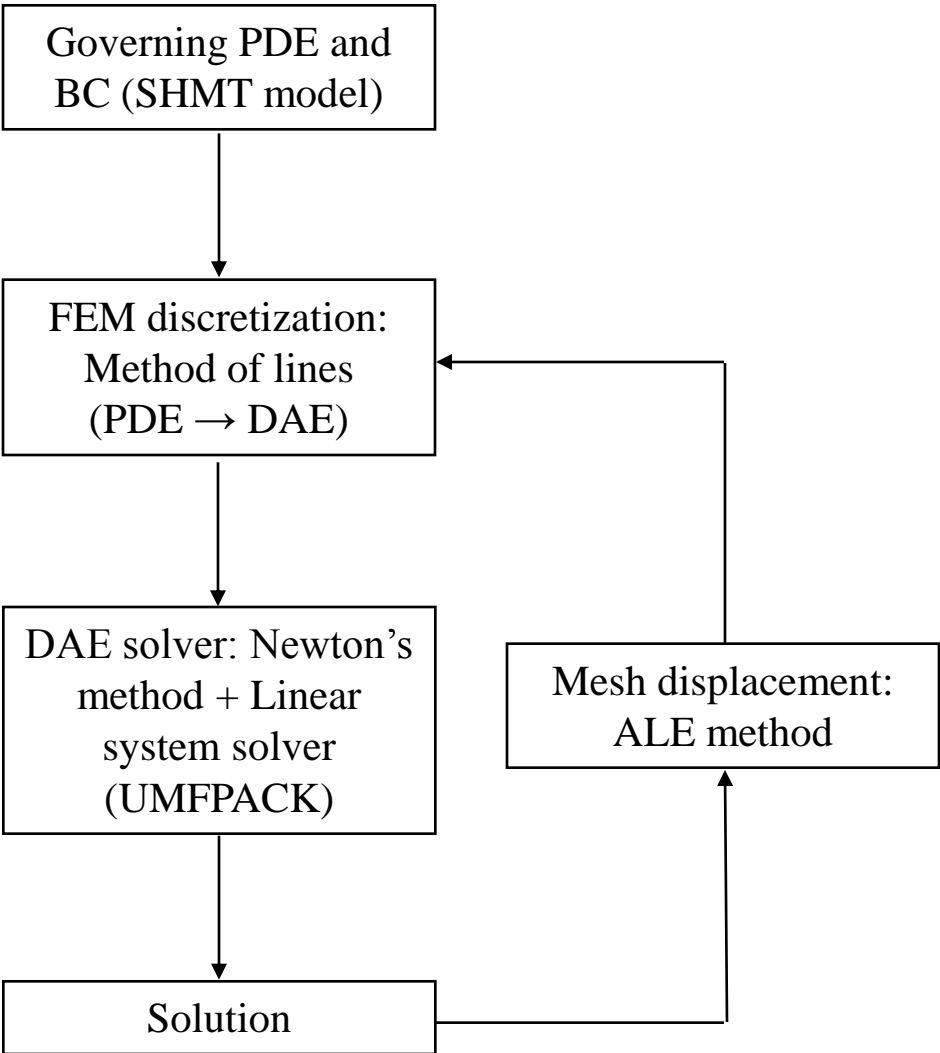


Figure 3 – Purlis and Salvadori

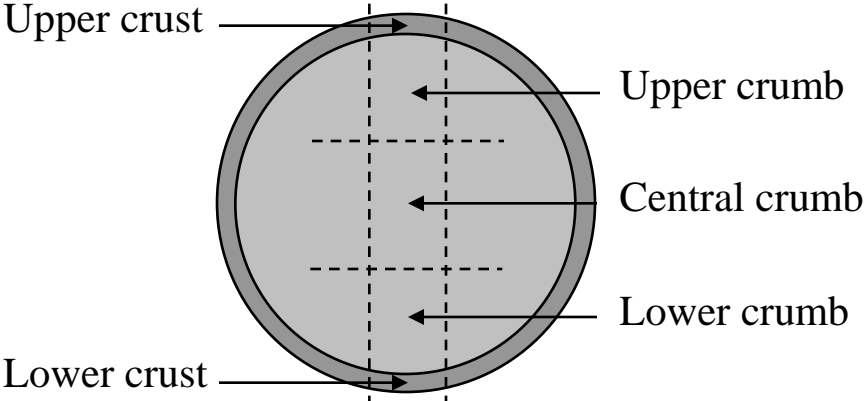


Figure 4 – Purlis and Salvadori

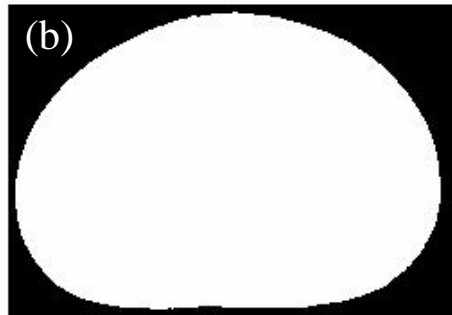


Figure 5 – Purlis and Salvadori

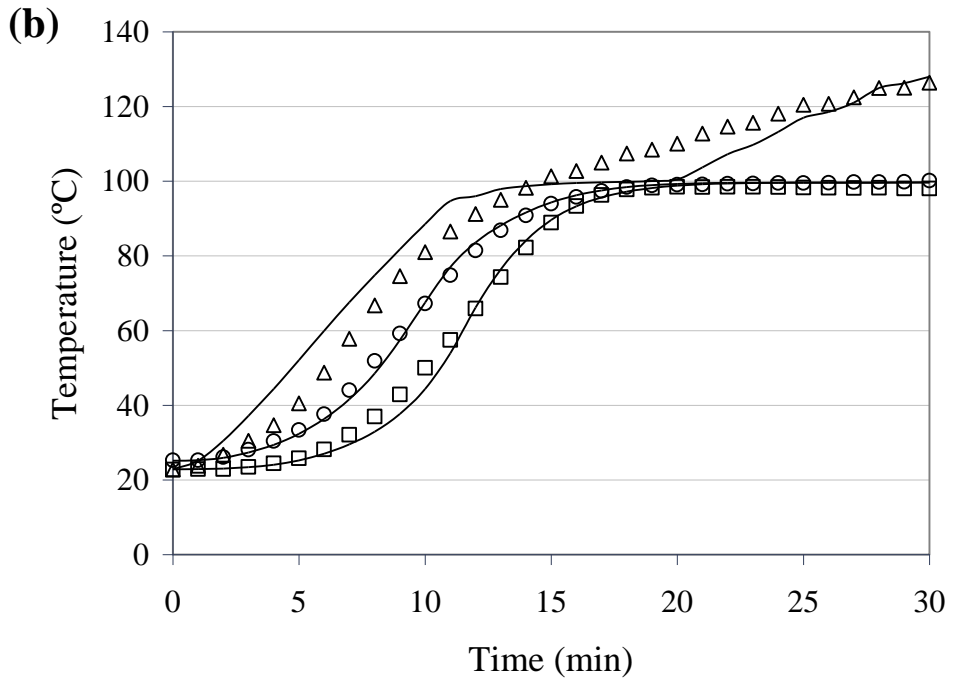
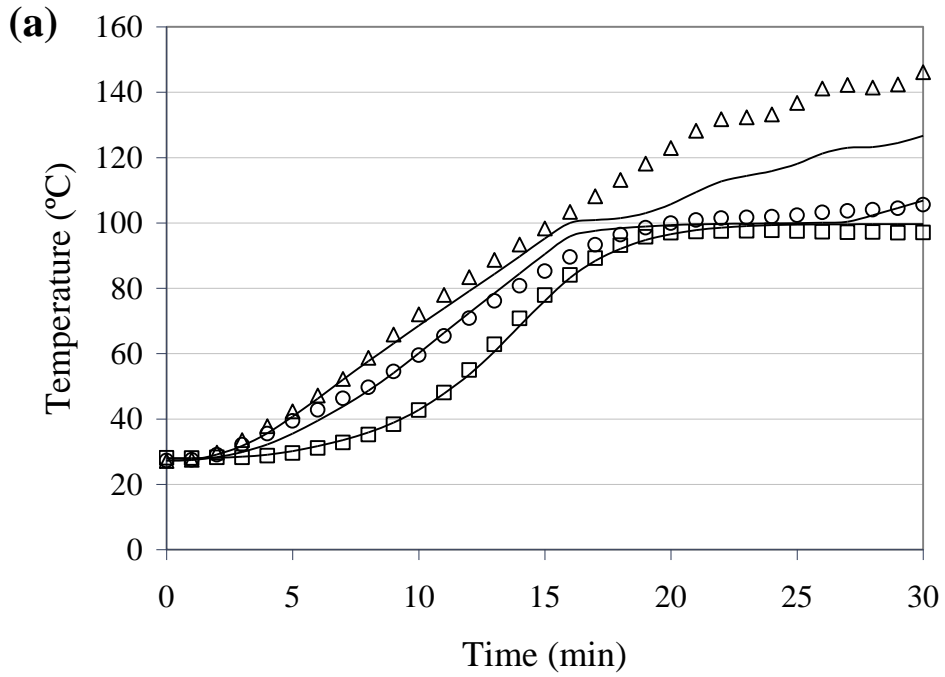


Figure 6 – Purlis and Salvadori

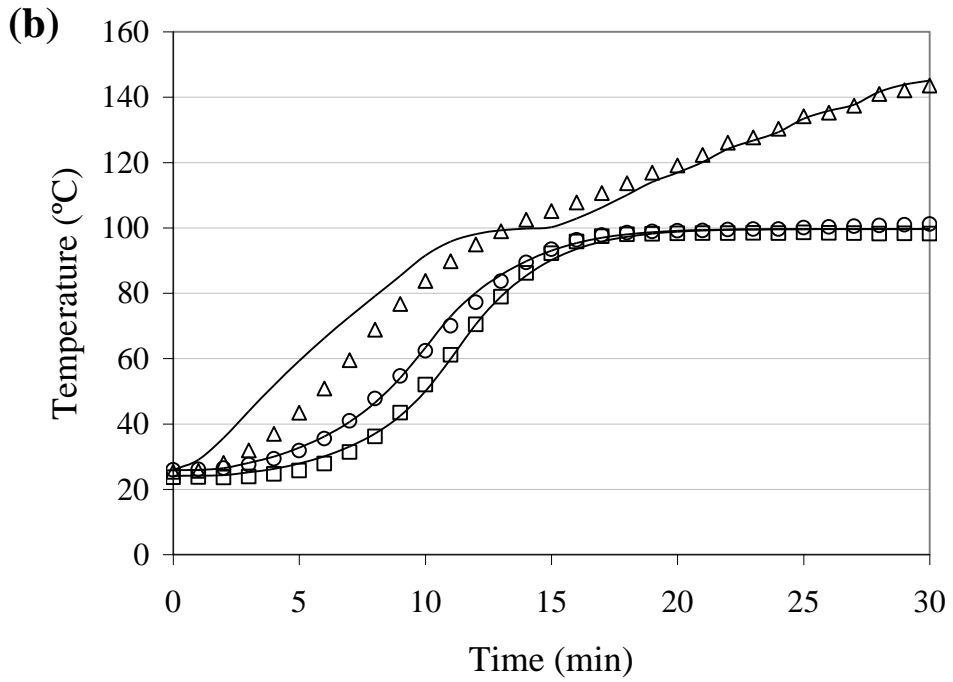
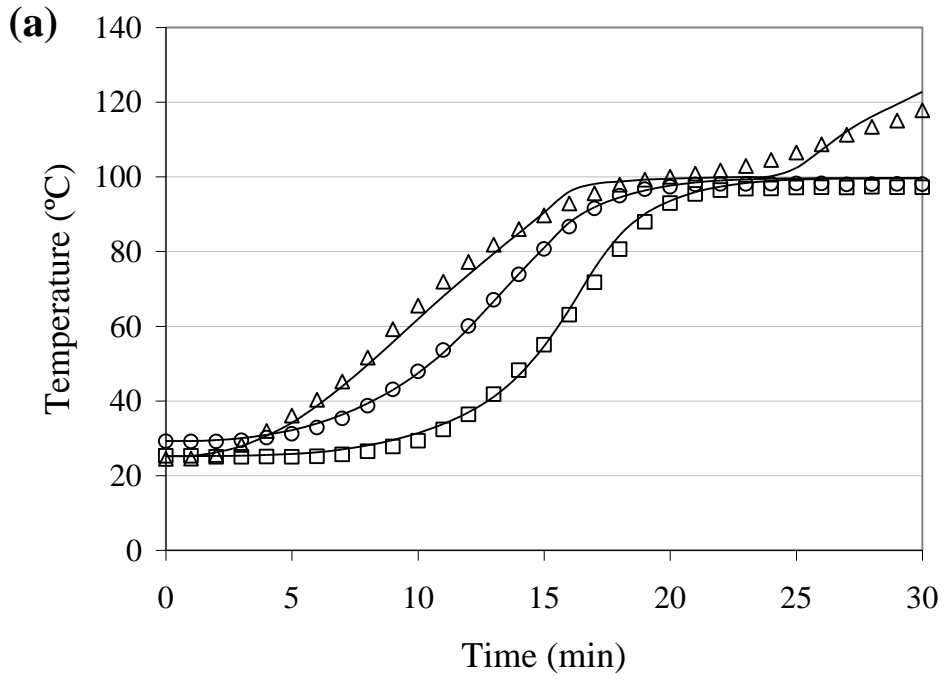


Figure 7 – Purlis and Salvadori

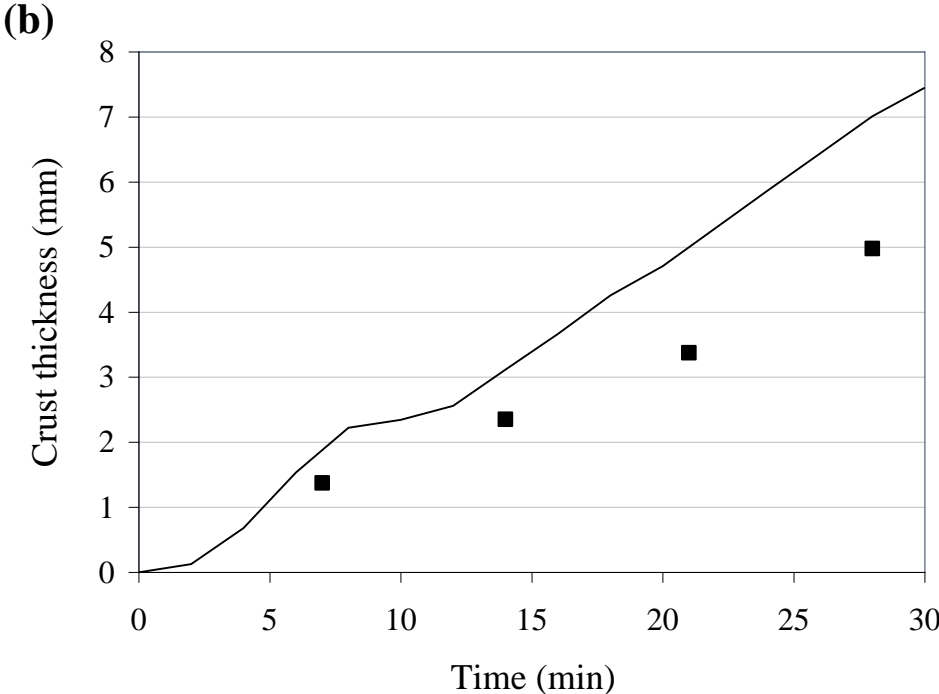
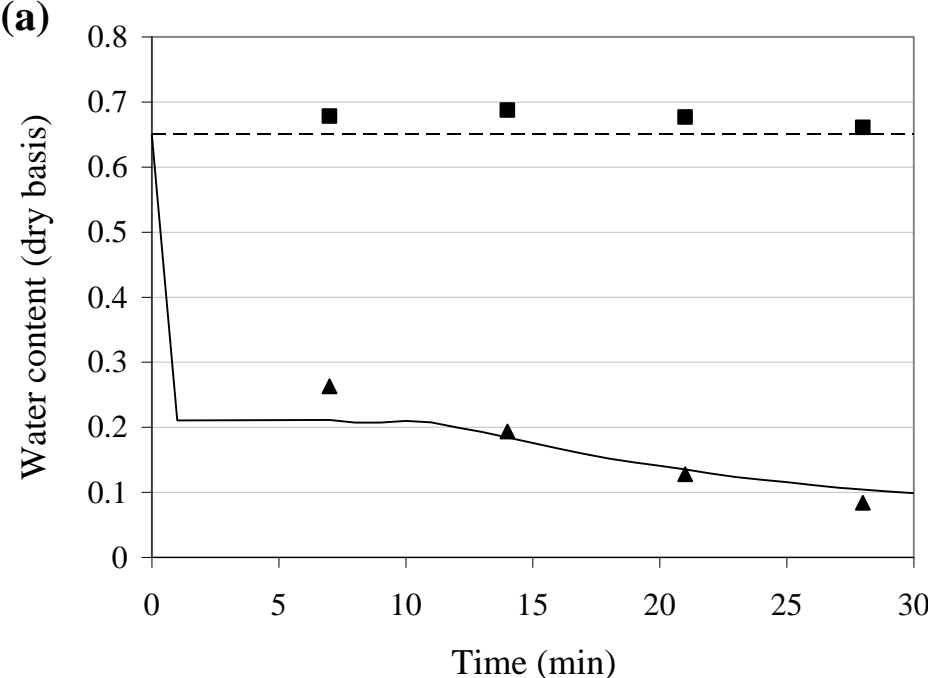


Figure 8 – Purlis and Salvadori

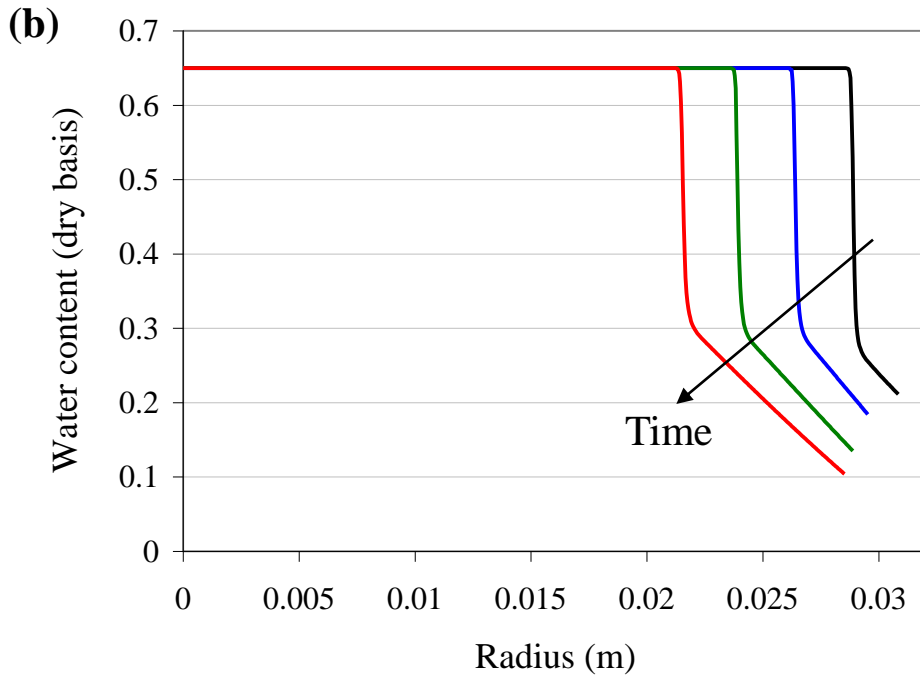
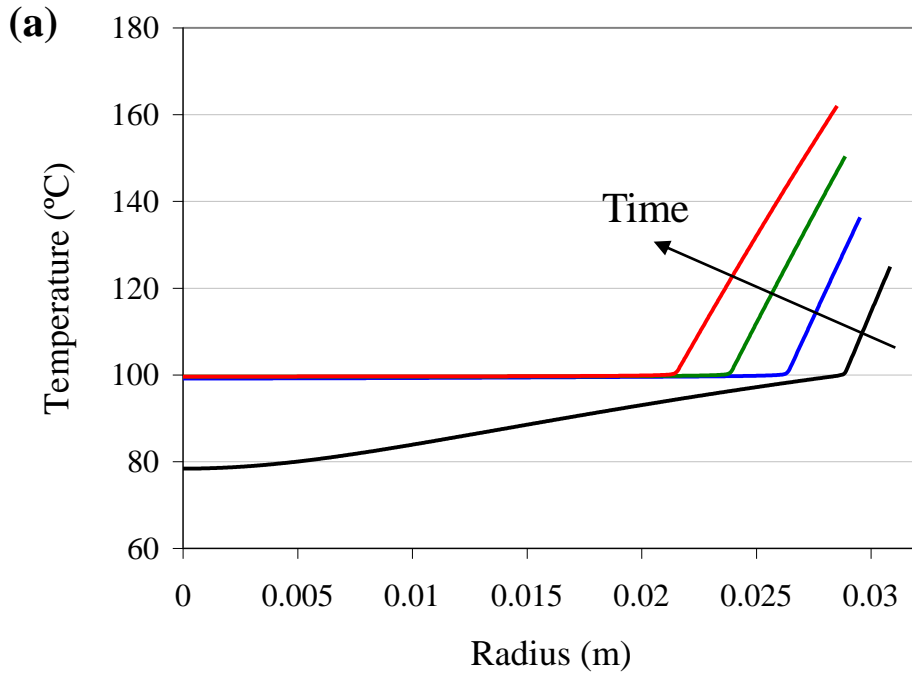


Figure 9 – Purlis and Salvadori

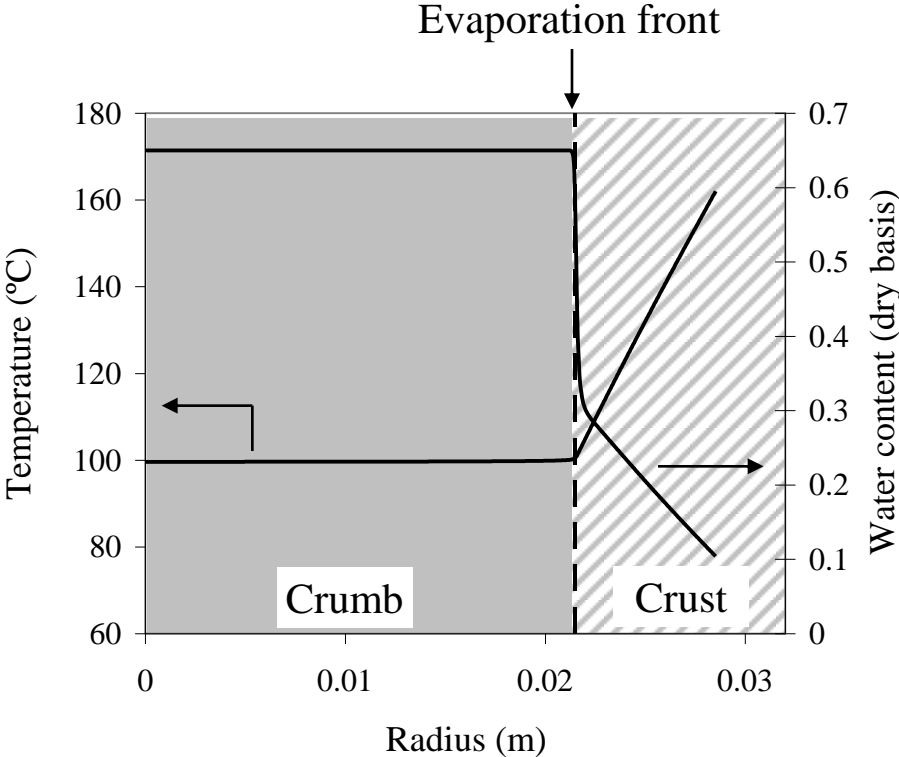


Figure 10 – Purlis and Salvadori

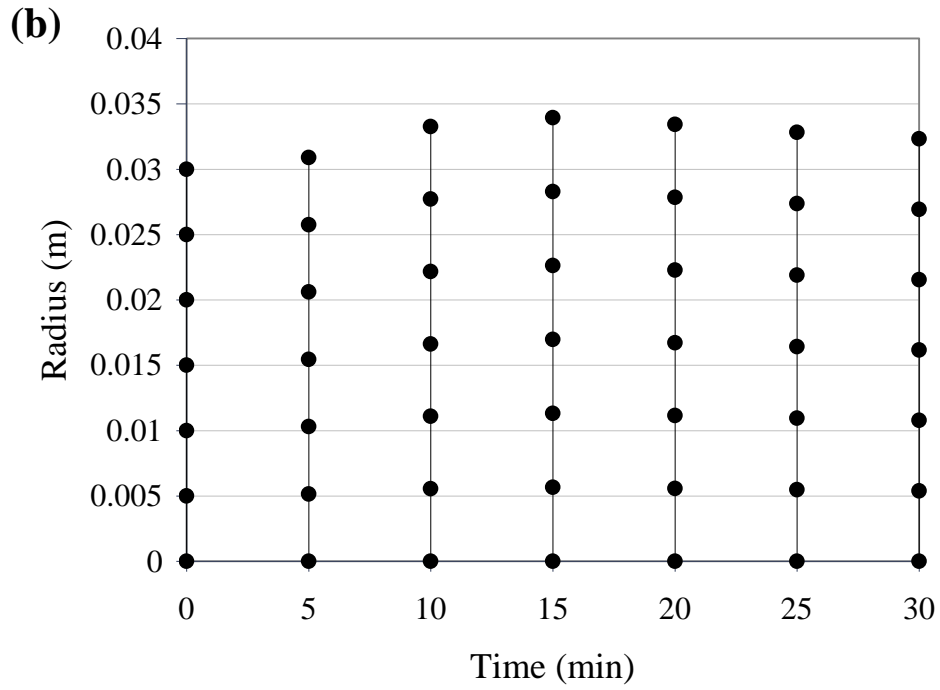
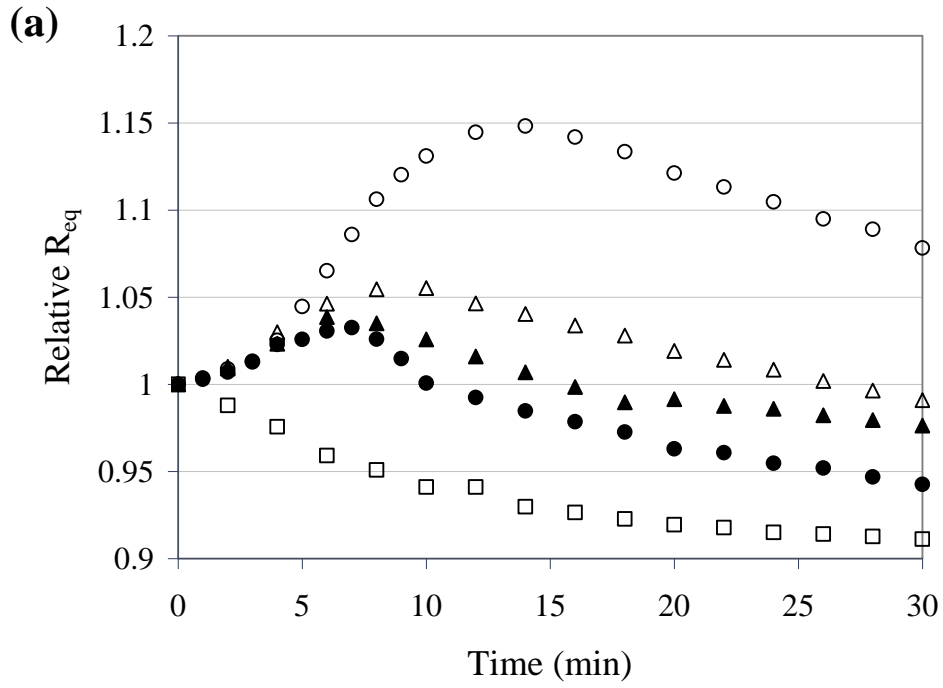


Figure 11 – Purlis and Salvadori

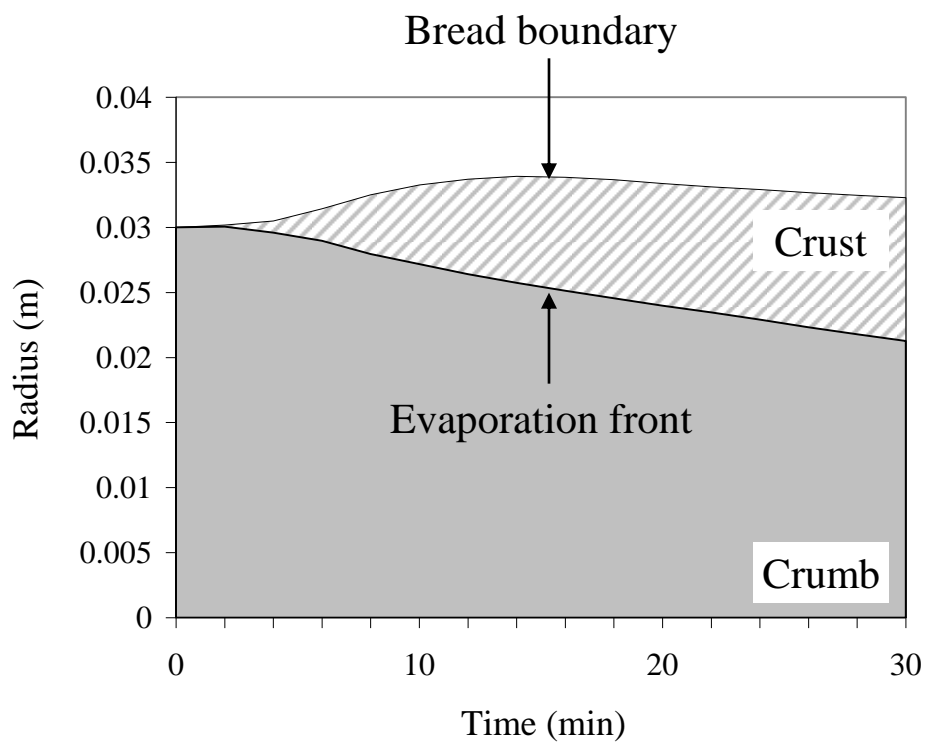


Figure 12 – Purlis and Salvadori

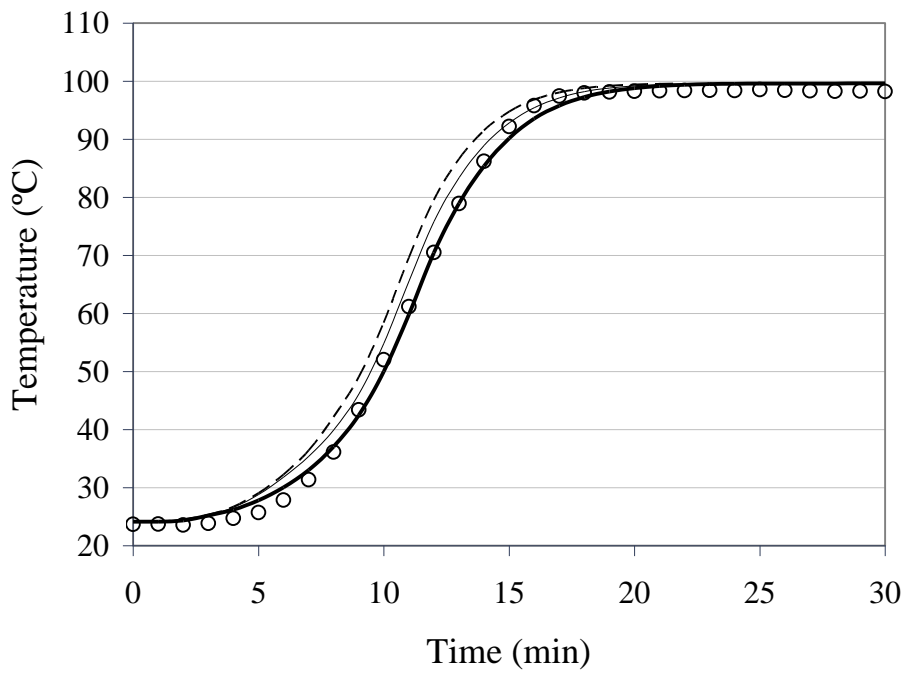


Table 1

Values for heat (h , in $\text{W m}^{-2} \text{K}^{-1}$) and mass (k_g , in $\text{kg Pa}^{-1} \text{m}^{-2} \text{s}^{-1}$) transfer coefficients (Purlis & Salvadori, 2009b).

Baking temperature ($^{\circ}\text{C}$)	Natural convection		Forced convection	
	h	k_g	h	k_g
200	7.68	3.38×10^{-9}	11.96	8.46×10^{-9}
220	7.95	6.04×10^{-9}	11.97	8.46×10^{-9}

Table 2

Mean absolute percentage error (e_{abs} , Eq. (34)) for temperature prediction (profiles shown in Figures 5 and 6). For a 30 min process, $n = 360$ since sampling time was 5 sec. Standard deviation is shown in parentheses. NC: natural convection; FC: forced convection.

Location	200 °C, NC	220 °C, NC	200 °C, FC	220 °C, FC
Core	1.53 (0.91)	2.67 (1.87)	2.59 (3.45)	2.32 (2.19)
Intermediate	3.18 (2.66)	1.30 (0.94)	1.37 (1.70)	1.16 (1.11)
Surface	7.61 (5.03)	2.85 (1.63)	8.37 (7.80)	9.53 (12.38)

Table 3

Experimental (EXP) and simulated (SIM) water content (dry basis) and thickness of bread crust during baking. Standard deviation is shown in parentheses. NC: natural convection; FC: forced convection.

Condition	Time (min)	Water content (kg kg ⁻¹)		Crust thickness (mm)	
		EXP	SIM	EXP	SIM
200 °C, NC	10	0.24 (0.02)	0.26	1.3 (0.1)	2.1
	20	0.13 (0.01)	0.23	2.8 (0.4)	4.0
	30	0.09 (0)	0.16	4.0 (0.4)	6.5
220 °C, NC	7	0.26 (0.06)	0.21	1.4 (0.3)	1.9
	14	0.19 (0.03)	0.18	2.4 (0.5)	3.1
	21	0.13 (0)	0.14	3.4 (0.8)	5.0
	28	0.08 (0.03)	0.10	5.0 (0.8)	7.0
200 °C, FC	10	0.23 (0)	0.15	1.8 (0.1)	3.4
	20	0.14 (0.03)	0.11	3.4 (0.2)	5.6
	30	0.10 (0)	0.09	4.1 (0.1)	7.6
220 °C, FC	7	0.23 (0.05)	0.14	1.6 (0.4)	3.5
	14	0.16 (0.03)	0.08	2.6 (0.3)	8.2
	21	0.12 (0)	0.07	3.6 (0.5)	9.6
	28	0.09 (0.01)	0.06	4.7 (0.6)	10.7